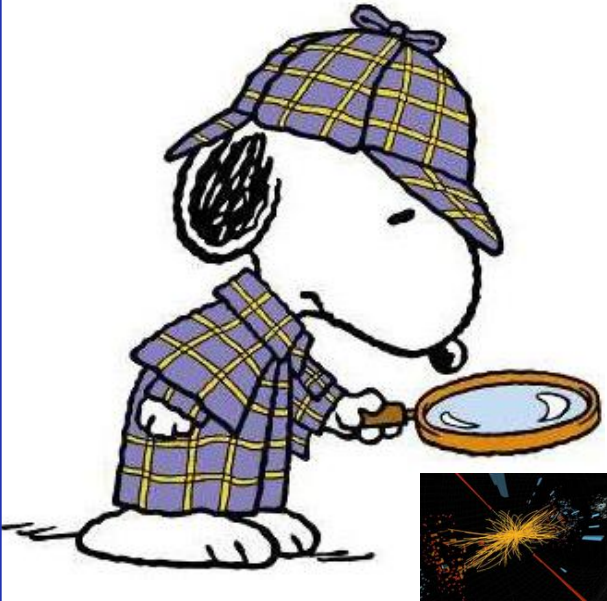


Search for $H \rightarrow c\bar{c}$ and Evidence of $H \rightarrow b\bar{b}$ in VBF Production with the ATLAS Detector

Austin Charles Mullins

Southern Methodist University
On behalf of the ATLAS Collaboration

39th Les Rencontres de Physique de la Vallée d'Aoste
La Thuile
March 4th, 2026



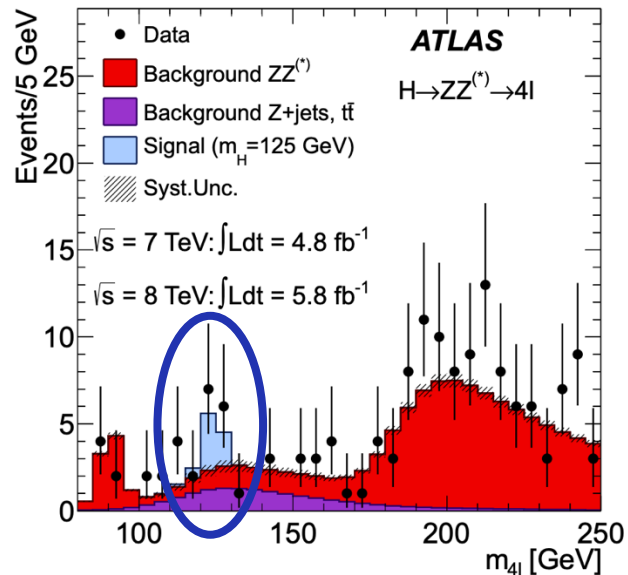
SMU[®]



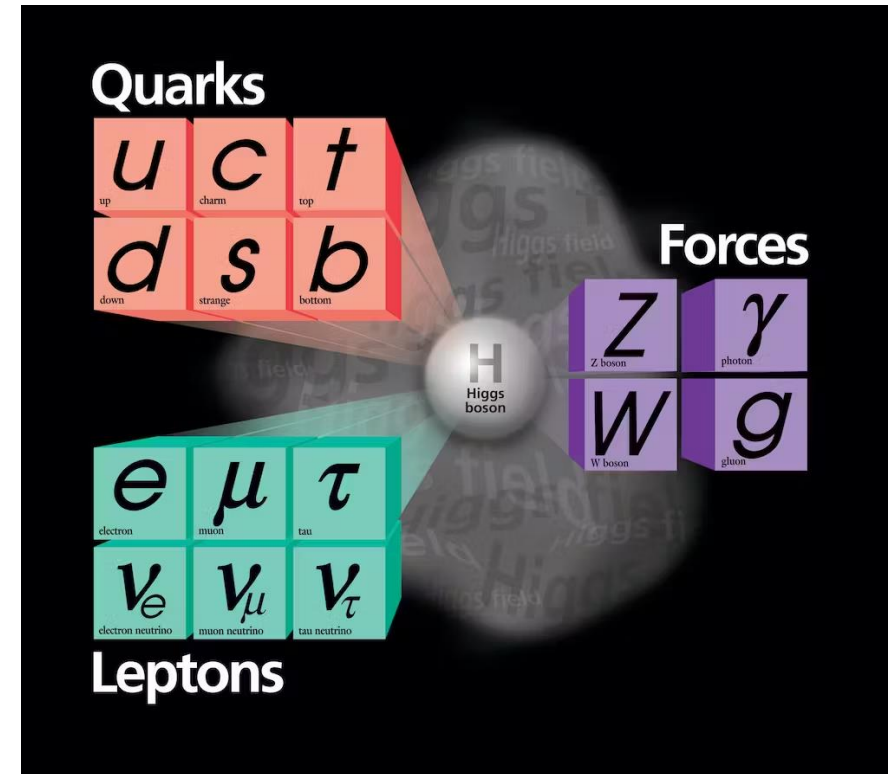
The Higgs Boson in a Nutshell

- Central to the Standard Model (SM) of particle physics
- The Higgs' Role: Interacts with all massive particles
 - Higgs mechanism provides a framework for electroweak symmetry breaking (EWSB)
 - EWSB is associated with the acquisition of mass by fundamental particles
- Higgs couples strongly to third generation fermions – well tested
- Higgs coupling to second generation fermions much less tested

[Phys. Lett. B 716 \(2012\) 1-29](#)

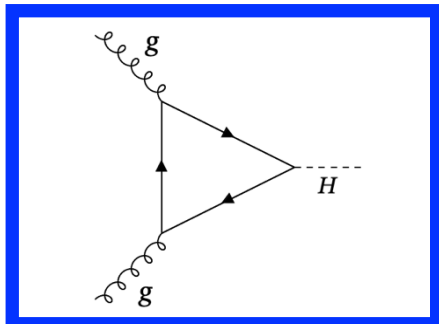


Run 1 Discovery of the Higgs Boson: $m_H = 125.38 \pm 0.41$ GeV

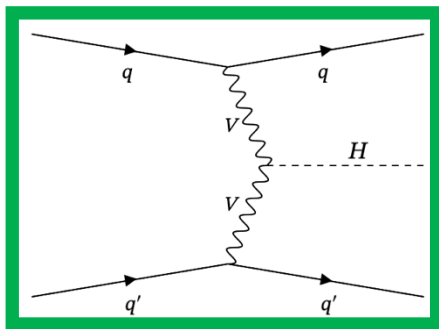


Higgs Production at the LHC

Production

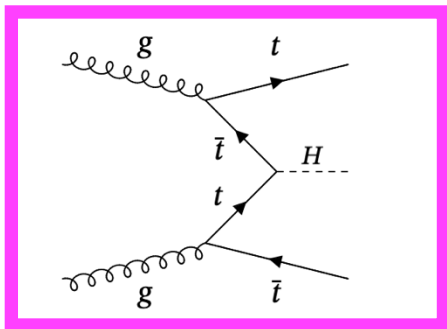


ggH

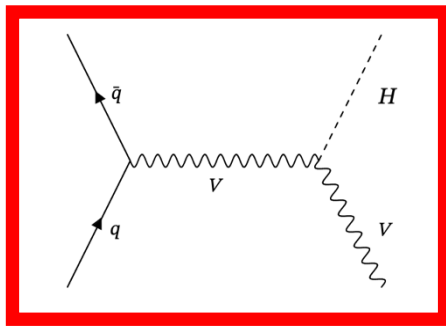


VBF

ttH



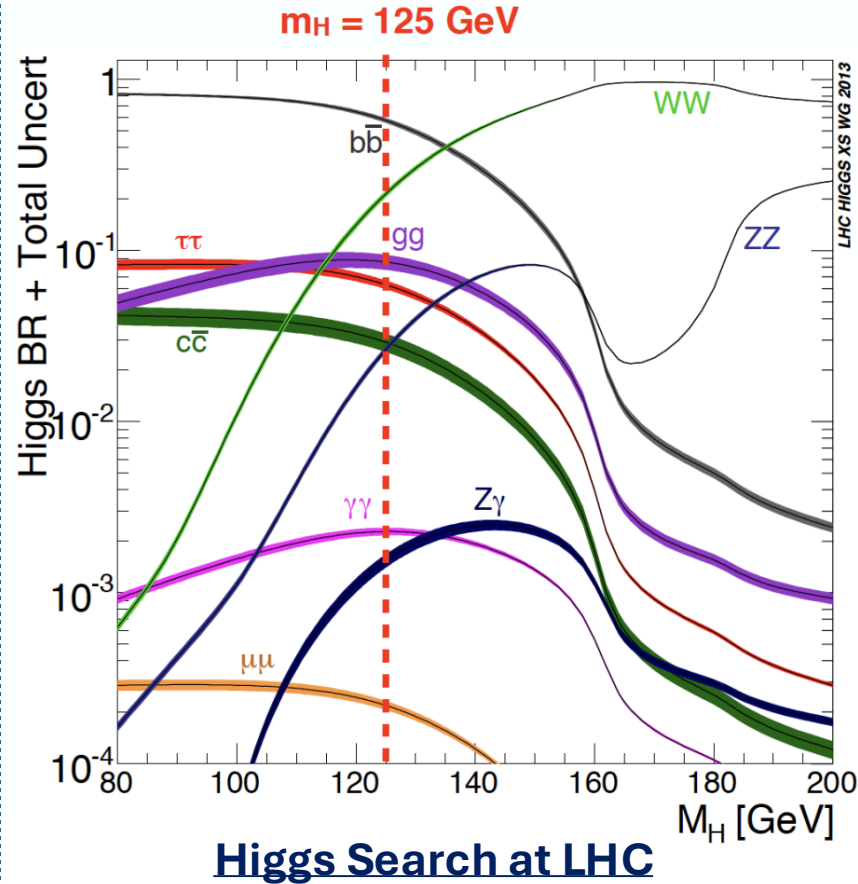
VH



Increasing signal purity
(for hadronic decays)

Decreasing
cross-section

Decay



Production	Run 2 # of Higgs
ggH	7M
VBF	500K
VH	300K
ttH	70K

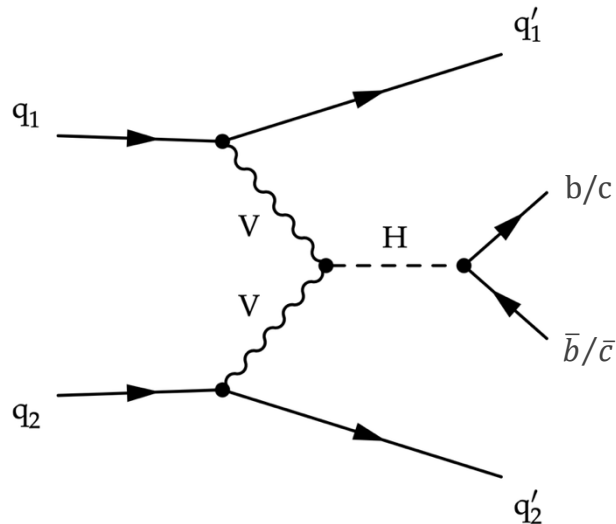
Decay	BR %
bb	58%
WW	21%
$\tau\tau$	6%
cc	3%
$\gamma\gamma$	0.2%

Motivation for VBF $H \rightarrow c\bar{c}/b\bar{b}$

- First search for $H \rightarrow c\bar{c}$ in the VBF production mode.
- Addition of VBF $H \rightarrow b\bar{b}$ measurement to increase the significance of VBF $H(b\bar{b})$.
- 2018 installation of **NEW** inclusive VBF trigger makes searching for VBF $H(c\bar{c})$ possible.
- **NEW** b- and c-tagger, GN2v01, with improvement in flavor tagging.

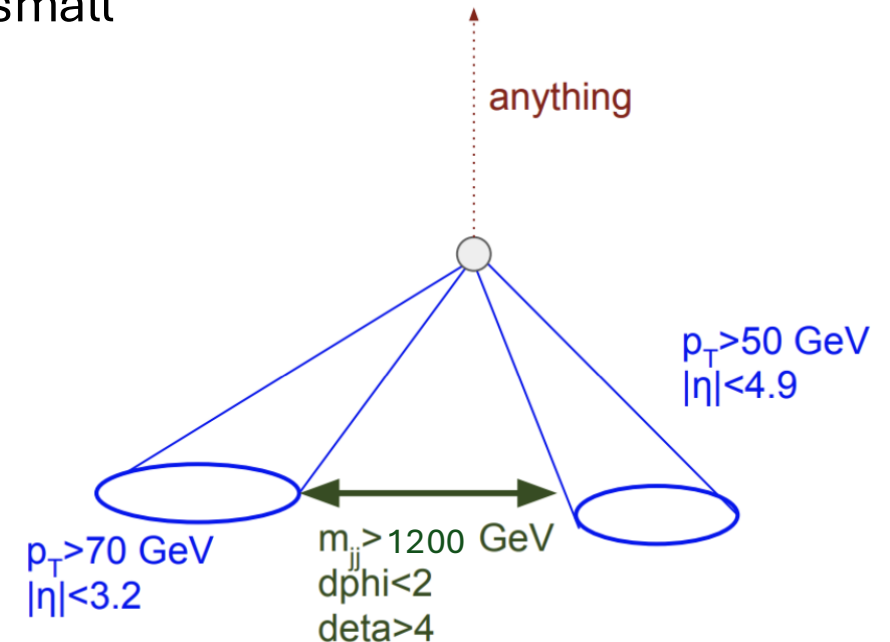
→ Analysis Strategy:

- Large focus on multijet background estimation due to small signals on top of dominant multijet background.

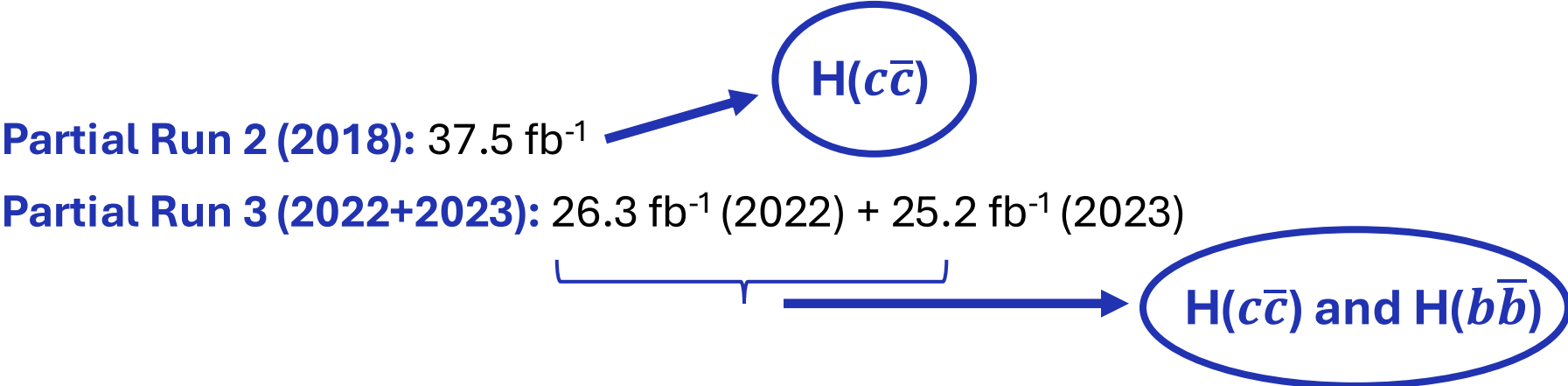


VBF candidate jets selection	
j_1	$p_T > 75 \text{ GeV}$ and $ \eta < 3.2$
j_2	$p_T > 75 \text{ GeV}$ and $ \eta < 4.5$
m_{jj}	$> 1200 \text{ GeV}$
$ \Delta\phi_{jj} $	< 2
$ \Delta\eta_{jj} $	> 4
In case of multiple jets satisfying these criteria, the pair maximizing m_{jj} is selected	
Higgs jets selection	
j_{h1}	$p_T > 20 \text{ GeV}$ and $ \eta < 2.5$ (and not selected as VBF jet)
j_{h2}	$p_T > 20 \text{ GeV}$ and $ \eta < 2.5$ (and not selected as VBF jet)
$ \Delta\phi_{j_h j_h} $	< 2
$p_{T,j_h j_h}$	$> 150 \text{ GeV}$
In case of multiple jets satisfying these criteria, the pair maximizing $p_{T,j_h j_h}$ is selected	
Veto	
Events with one or more isolated electrons or muons are rejected	
Flavor tagging	
$H \rightarrow b\bar{b}$ channel	j_{h1} and j_{h2} are b-tagged with 77% b-tagging efficiency
$H \rightarrow c\bar{c}$ channel	j_{h1} and j_{h2} are not b-tagged and are c-tagged with 50% c-tagging efficiency

Inclusive VBF

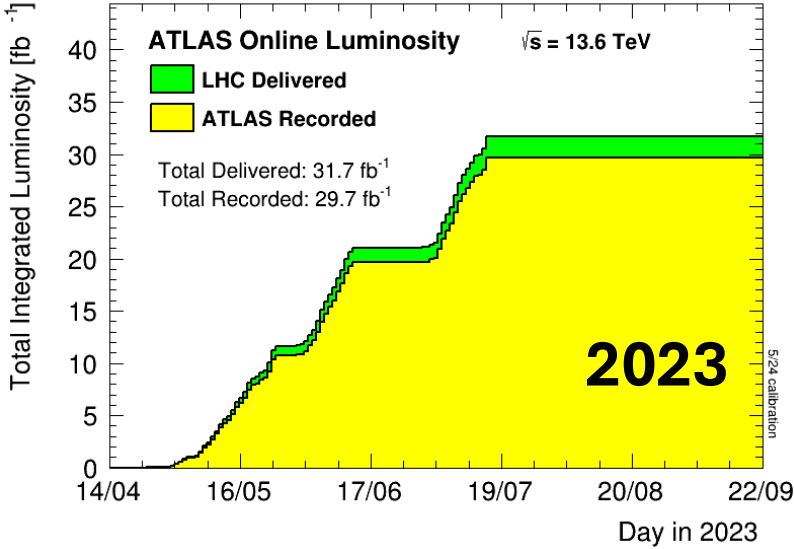
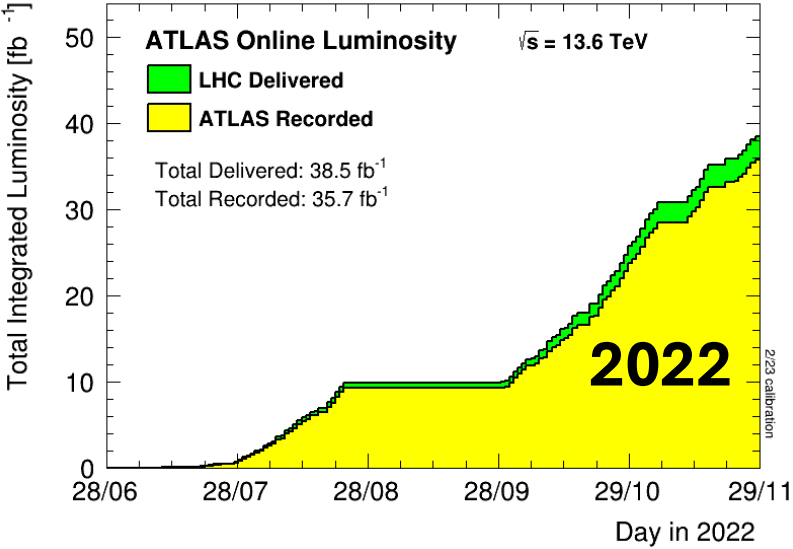
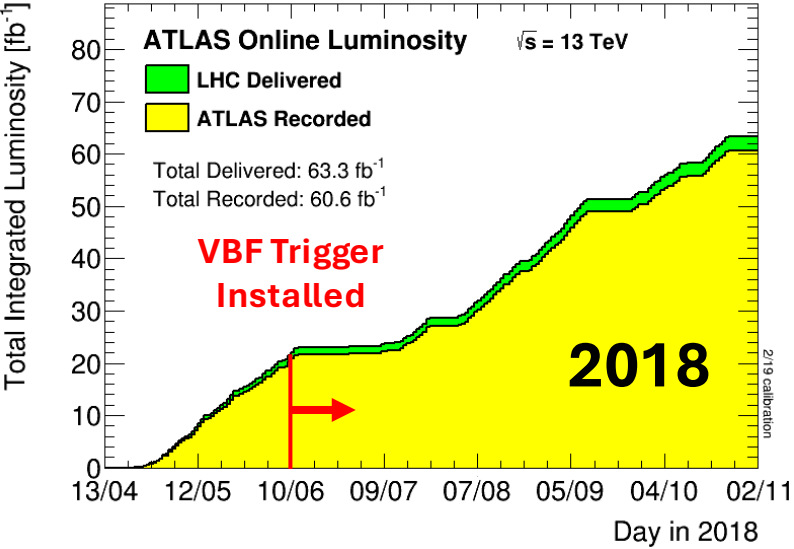


ATLAS Run 2 + Run 3 Data Summary



TOTAL DATA USED

- **H(c \bar{c}): 89 fb⁻¹**
- **H(b \bar{b}): 51.5 fb⁻¹**



Improvements in Flavour Tagging

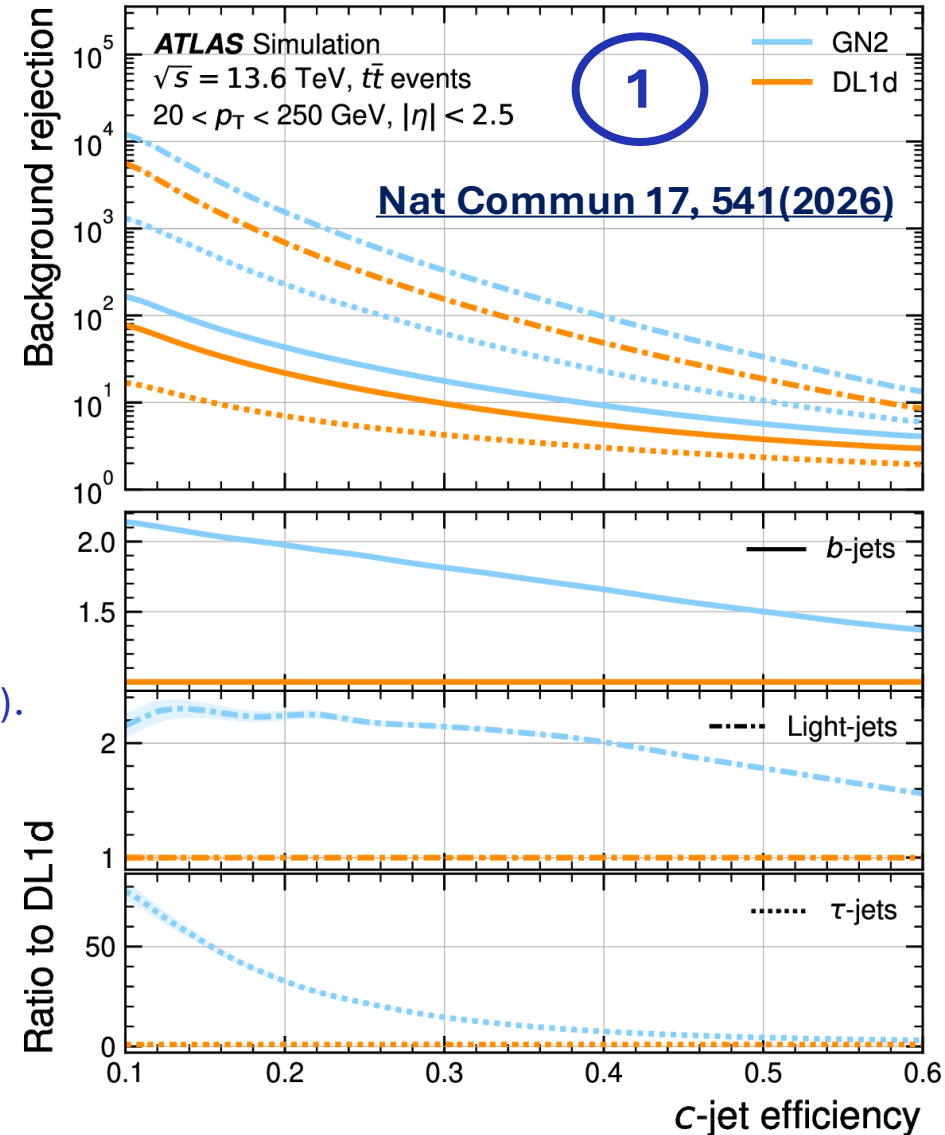
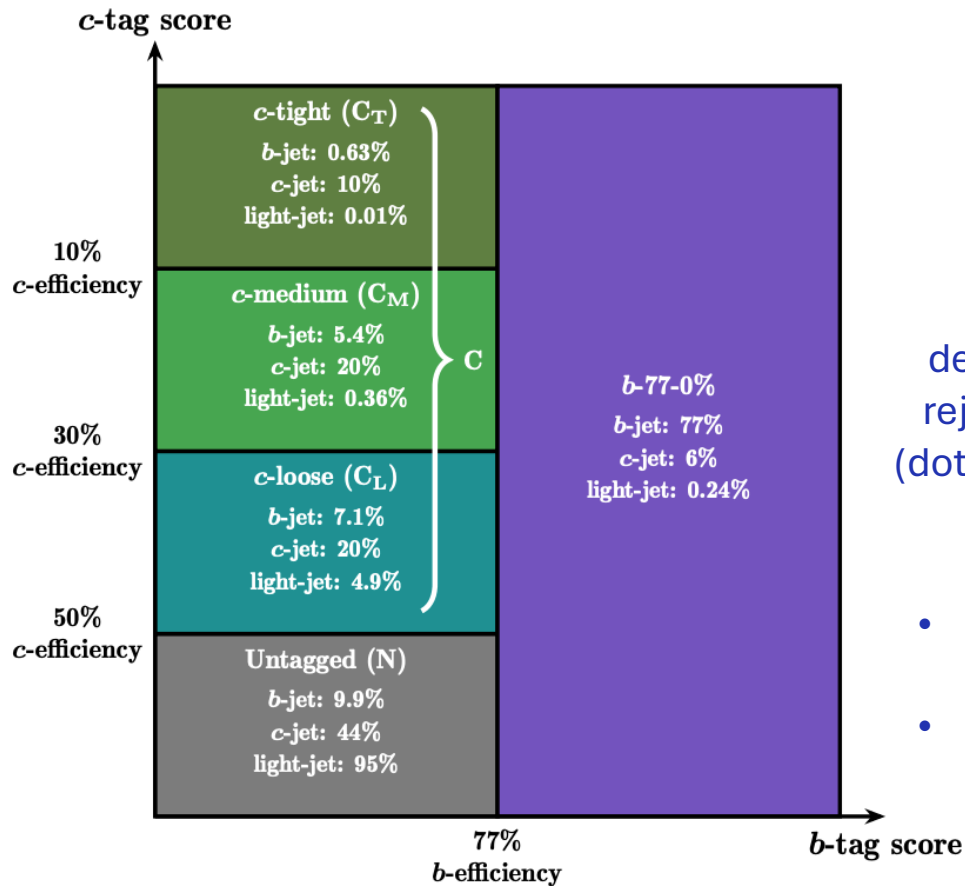
GN2 makes searching for $H \rightarrow c\bar{c}$ in the VBF production mode possible.

GN2 see's major improvement in background rejection compared to previous DL1d tagger.

1

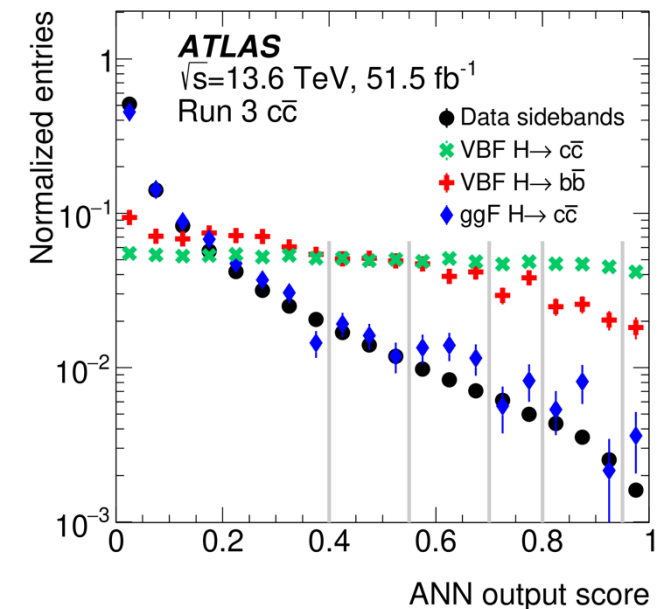
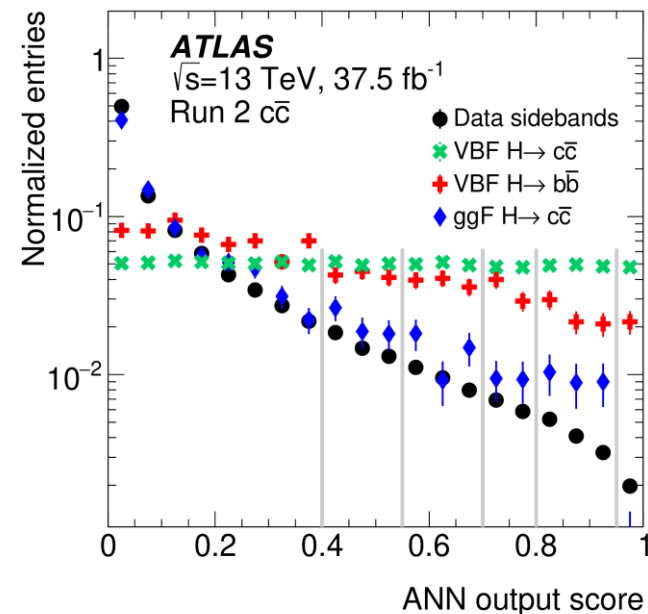
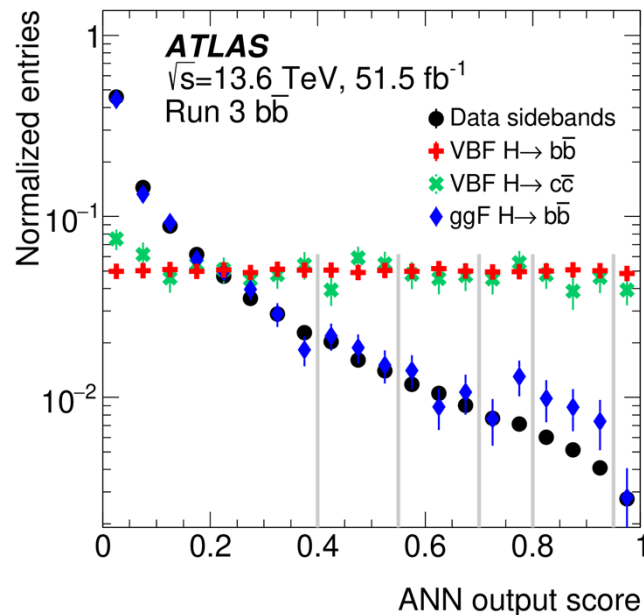
c-jet efficiency ROC curves demonstrating GN2's background rejection of b-jets (solid), light-jets (dotted-dashed), and τ -jets (dashed).

- Jet must pass **77%** working point to be **b-tagged**.
- Jets that **fail 77% WP** but **pass 50% WP** are **c-tagged**.

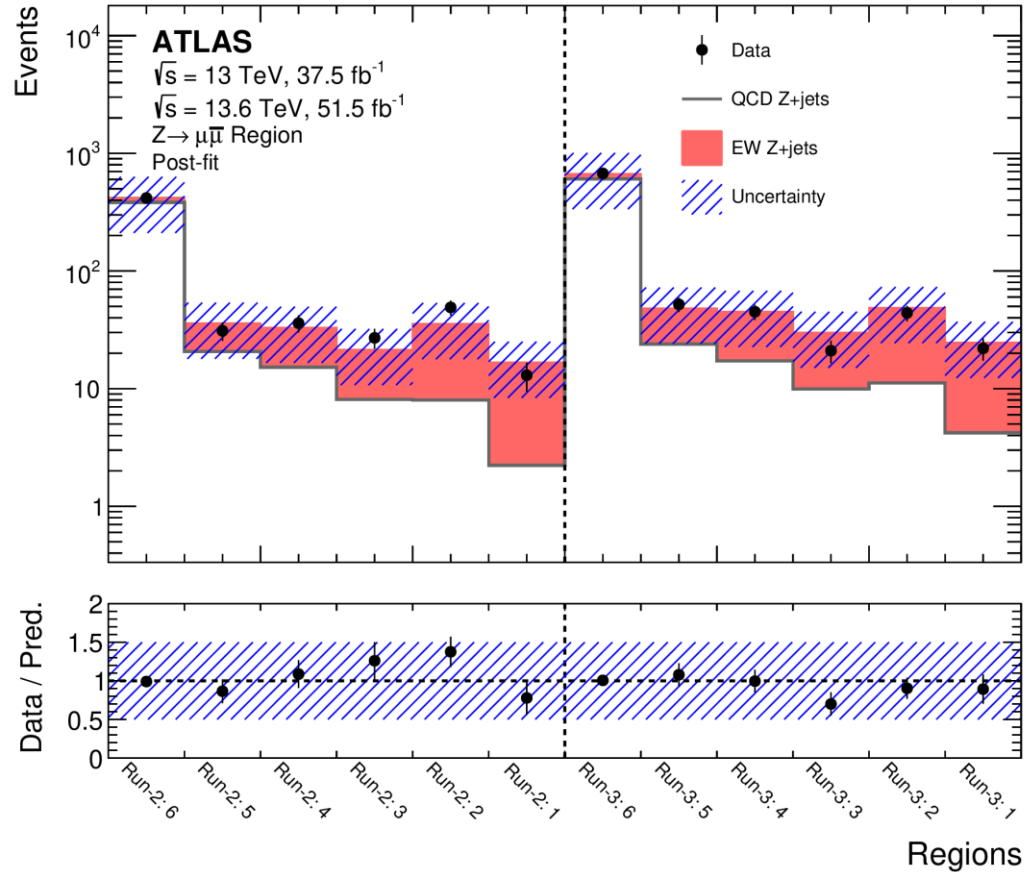


Analysis Strategy - ANN

- Adversarial neural network's (ANNs) are trained to obtain signal (s) vs. background (b) discriminant.
- Classifier is used to categorize events into more s-like or more b-like regions (6 total signal regions) and the $m_{jh,jh}$ is fit in each region simultaneously.
- Signal events are taken from VBF MC samples, background events are taken from data sidebands on either side of Higgs mass window ($100 < m_{jh,jh} < 140$ GeV) but within range $50 < m_{jh,jh} < 200$ GeV.
- SR6 is signal depleted and dominated by non-resonant multijet background, SR1 is signal enriched.



Analysis Strategy - $Z \rightarrow \mu\bar{\mu}$ CR

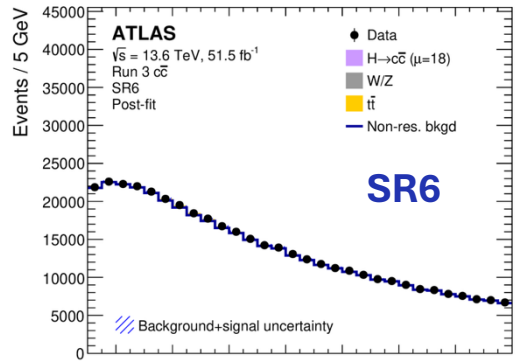


Post-fit $Z \rightarrow \mu\bar{\mu}$ yields in the ANN SR regions used to extract norm factors for V+jets backgrounds.

- **Dedicated $Z \rightarrow \mu\bar{\mu}$ control regions (CRs) are defined to:**
 - Check subdominant resonant backgrounds.
 - Measure trigger efficiency.
- Same trigger and selection criteria applied.
- VBF jets selected adhere to the same requirements as those in the signal region.
- **50% normalization uncertainty** applied to V+jets backgrounds.
- **7% (4%) uncertainty** in the VBF trigger selection efficiency is applied to Run-2 (Run-3) simulated events.

$$\text{TriggerEfficiency} = \frac{\text{Events passing inclusive VBF trigger} + \text{muon trigger} + \text{offline selection}}{\text{Events passing muon trigger} + \text{offline selection}}$$

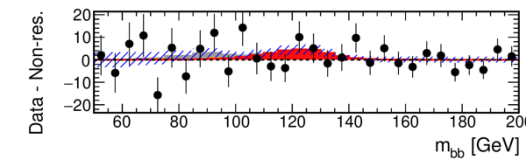
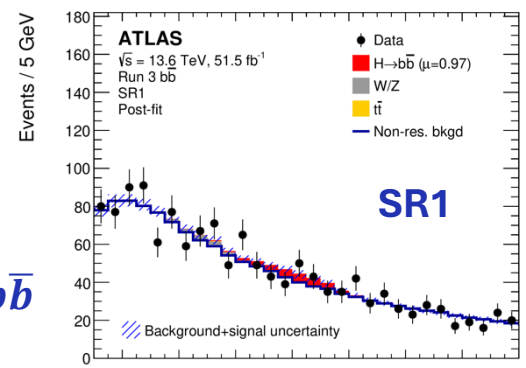
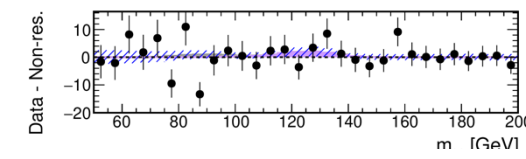
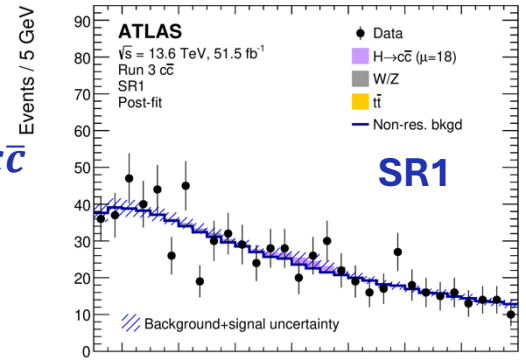
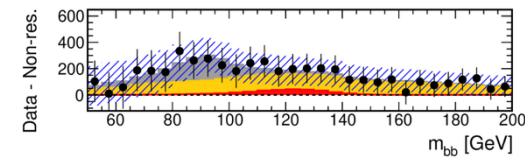
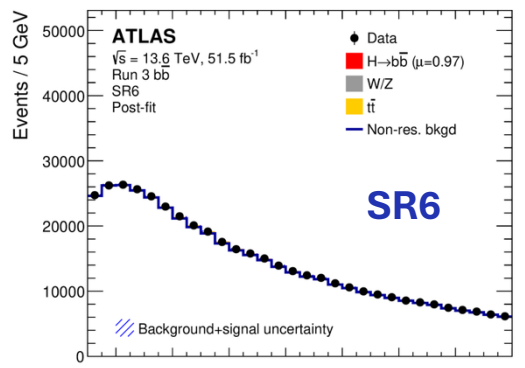
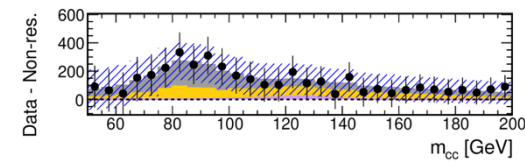
Post-Fit Distributions



VBF $H \rightarrow c\bar{c}$
 Run 3

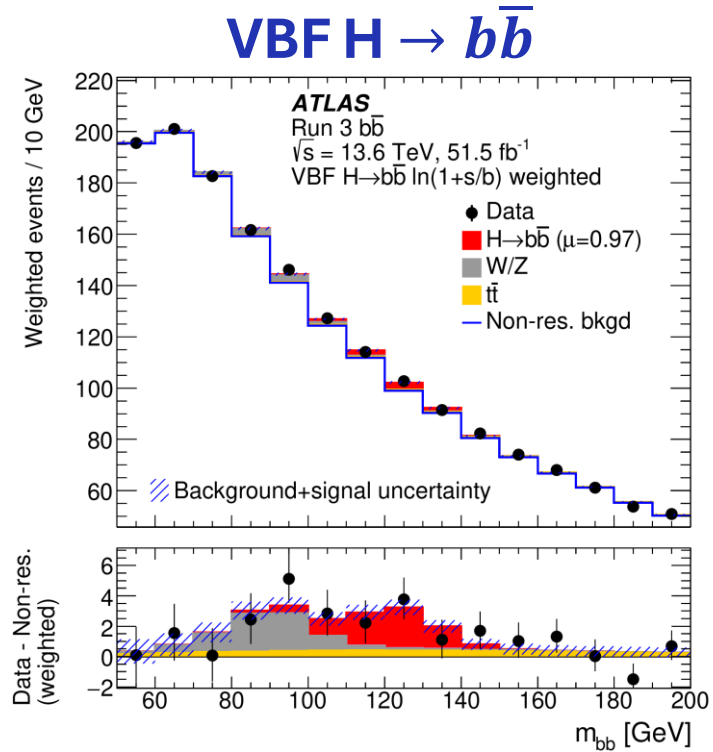
Extract Background
 Shape

VBF $H \rightarrow b\bar{b}$
 Run 3

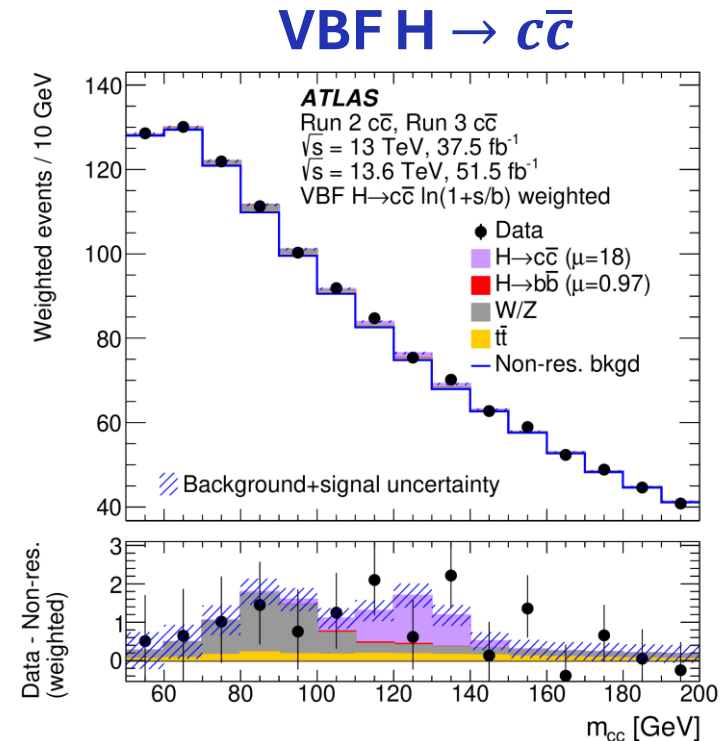


- Two systematic uncertainties introduced for possible non-res. bkgd shape differences between SRs derived from the data sidebands:
 - Residual uncertainties
 - Remaining correlations between ANN score and $m_{jh,jh}$.
 - Leads to slight difference in bkgd shapes between SR1-SR5.
 - Bias uncertainties
 - Training could inadvertently “sculpt” the bkgd shape in the mass window.
 - Could our ANN+non-res. bkgd extraction method create or hide signal excess in the mass window?

Higgs Candidate Jet Mass Distributions



$$\mu(H \rightarrow b\bar{b}): 0.97^{+0.57}_{-0.50}$$



$$\mu(H \rightarrow c\bar{c}): 18^{+13}_{-13}$$

Combination of SRs weight by $\ln(1+s/b)$ and summed for the $H \rightarrow c\bar{c}$ and $H \rightarrow b\bar{b}$ channels. Signal (s) is calculated based on the observed Higgs boson signal for each region and background (b) is calculated based on the post-fit background yields in each region.

Combination Results: $H \rightarrow b\bar{b}$

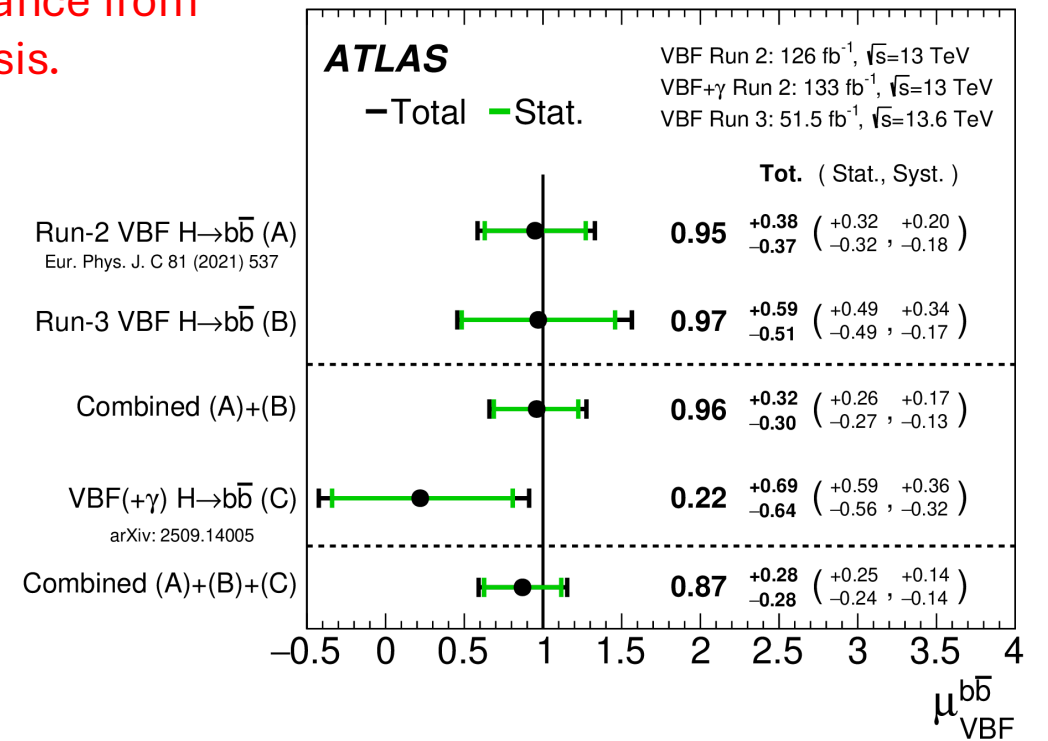
$\mu_{VBF}^{b\bar{b}}$ results for Run 2 + Partial Run 3
VBF and VBF(+ γ) $H \rightarrow b\bar{b}$ combination

Signal strength and significance from
the performed analysis.

VBF $H \rightarrow b\bar{b}$ Combination

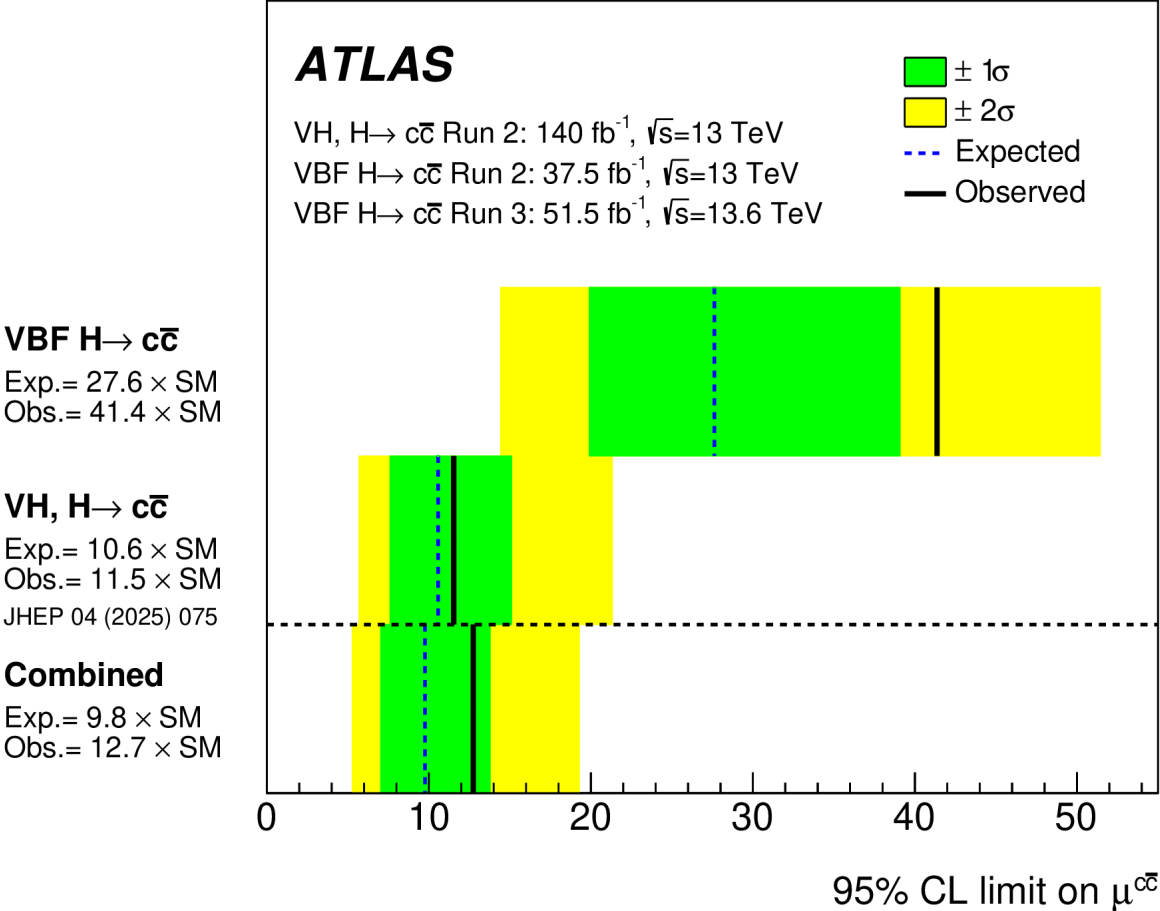
	Observed $\mu_{VBF}^{b\bar{b}}$	Expected significance	Observed significance
Run-2 VBF $H \rightarrow b\bar{b}$ (A)	$0.95^{+0.38}_{-0.37}$	2.8	2.6
Run-3 VBF $H \rightarrow b\bar{b}$ (B)	$0.97^{+0.59}_{-0.51}$	1.9	1.9
Combined (A)+(B)	$0.96^{+0.32}_{-0.30}$	3.3	3.3
VBF(+ γ) $H \rightarrow b\bar{b}$ (C)	$0.22^{+0.69}_{-0.64}$	1.4	0.3
Combined (A)+(B)+(C)	$0.87^{+0.28}_{-0.28}$	3.6	3.2

Signal strength and significance after
performing the combination.

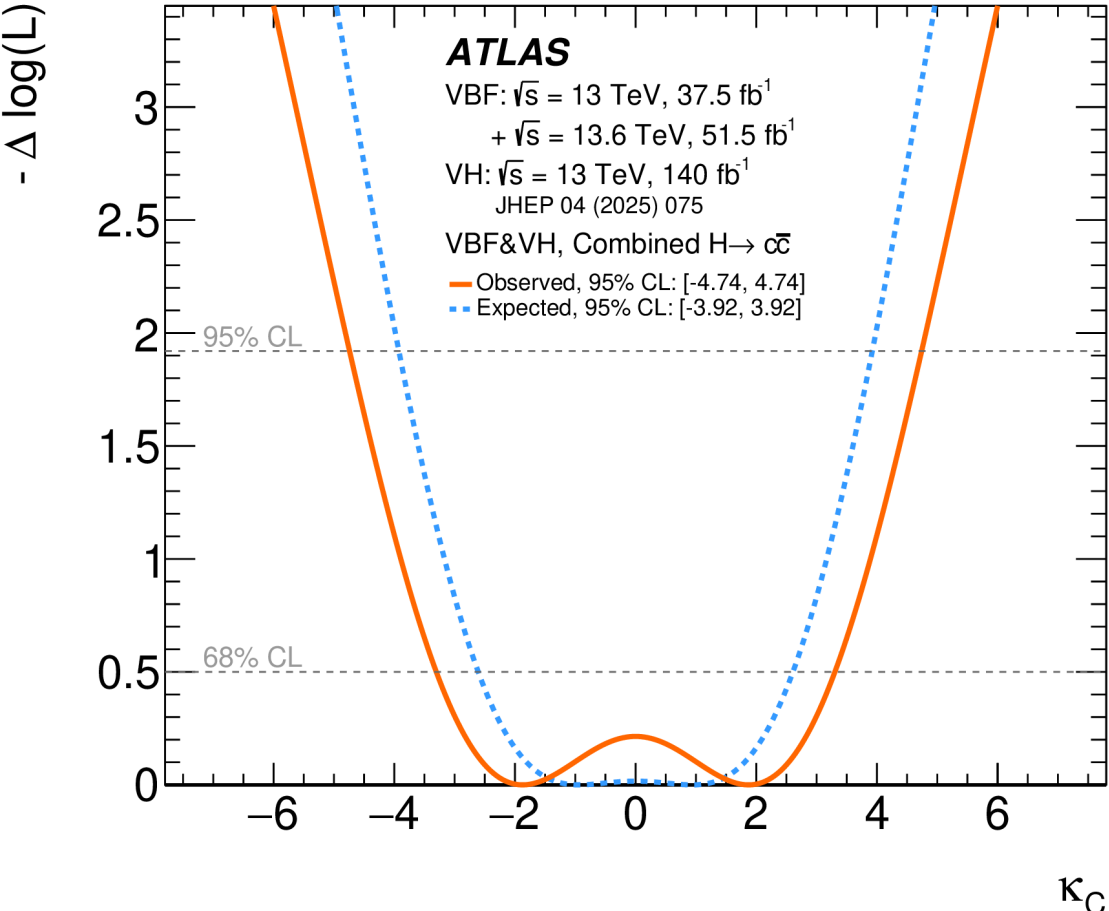


Observed (Expected) significance
of (A)+(B)+(C): **3.2 σ** (**3.6 σ**).

Combination Results: $H \rightarrow c\bar{c}$



Limits set on Run 2 + Run 3 VBF $H \rightarrow c\bar{c}$ and Run 2 VH $H \rightarrow c\bar{c}$ combined



Results of Run 2 + Run 3 VBF $H \rightarrow c\bar{c}$ and Run 2 VH $H \rightarrow c\bar{c}$ combined κ_c

Results Summary

❖ $H \rightarrow c\bar{c}/b\bar{b}$ via the VBF production mode was investigated using partial Run 2 and partial Run 3 datasets for a combined integrated luminosity of 89 fb^{-1} .

- $H \rightarrow b\bar{b}$

- $\mu(H \rightarrow b\bar{b})$: $0.97^{+0.57}_{-0.50}$
- **Observed(Expected)** of $\mu(H \rightarrow b\bar{b})$: 1.9σ (1.9σ)

- $H \rightarrow c\bar{c}$

- $\mu(H \rightarrow c\bar{c})$: 18^{+13}_{-13}
- **Observed(Expected)** upper limit on $\mu(H \rightarrow c\bar{c})$: 41 (28)

❖ Three combinations were performed: VBF $H \rightarrow b\bar{b}$ with VBF(+ γ) $H \rightarrow b\bar{b}$, and VBF $H \rightarrow c\bar{c}$ with VH $H \rightarrow c\bar{c}$.

- VBF $H \rightarrow b\bar{b}$ Combination

- $\mu(H \rightarrow b\bar{b})$: $0.96^{+0.32}_{-0.30}$
- **Observed(Expected)** significance of $\mu(H \rightarrow b\bar{b})$: 3.3σ (3.3σ)

- VBF $H \rightarrow b\bar{b}$ with VBF(+ γ) $H \rightarrow b\bar{b}$ Combination

- $\mu(H \rightarrow b\bar{b})$: $0.87^{+0.28}_{-0.28}$
- **Observed(Expected)** significance of $\mu(H \rightarrow b\bar{b})$: 3.2σ (3.6σ)

- VBF $H \rightarrow c\bar{c}$ and VH $H \rightarrow c\bar{c}$ Combination

- **Observed(Expected)** upper limit on $\mu(H \rightarrow c\bar{c})$: 13 (9.8)

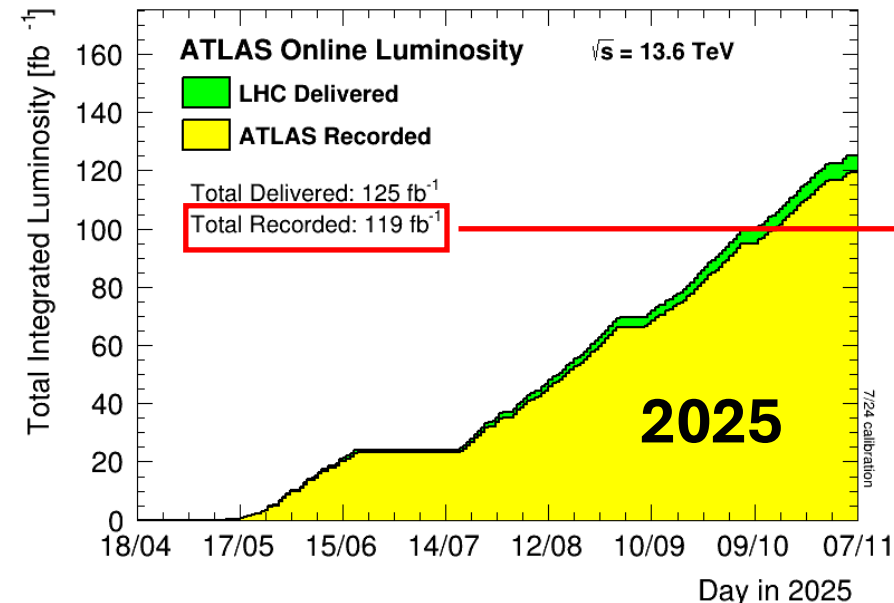
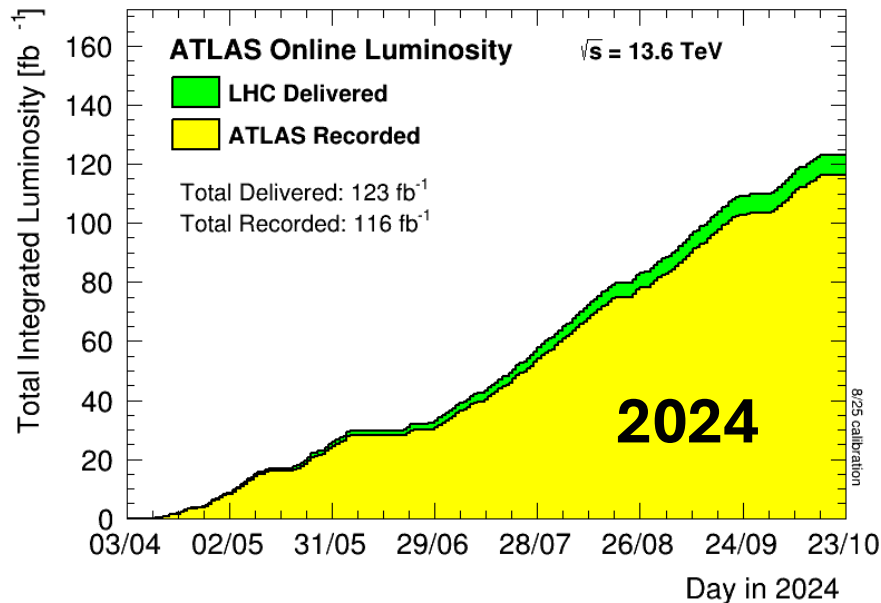
[READ OUR PAPER!](#)



SCAN ME!

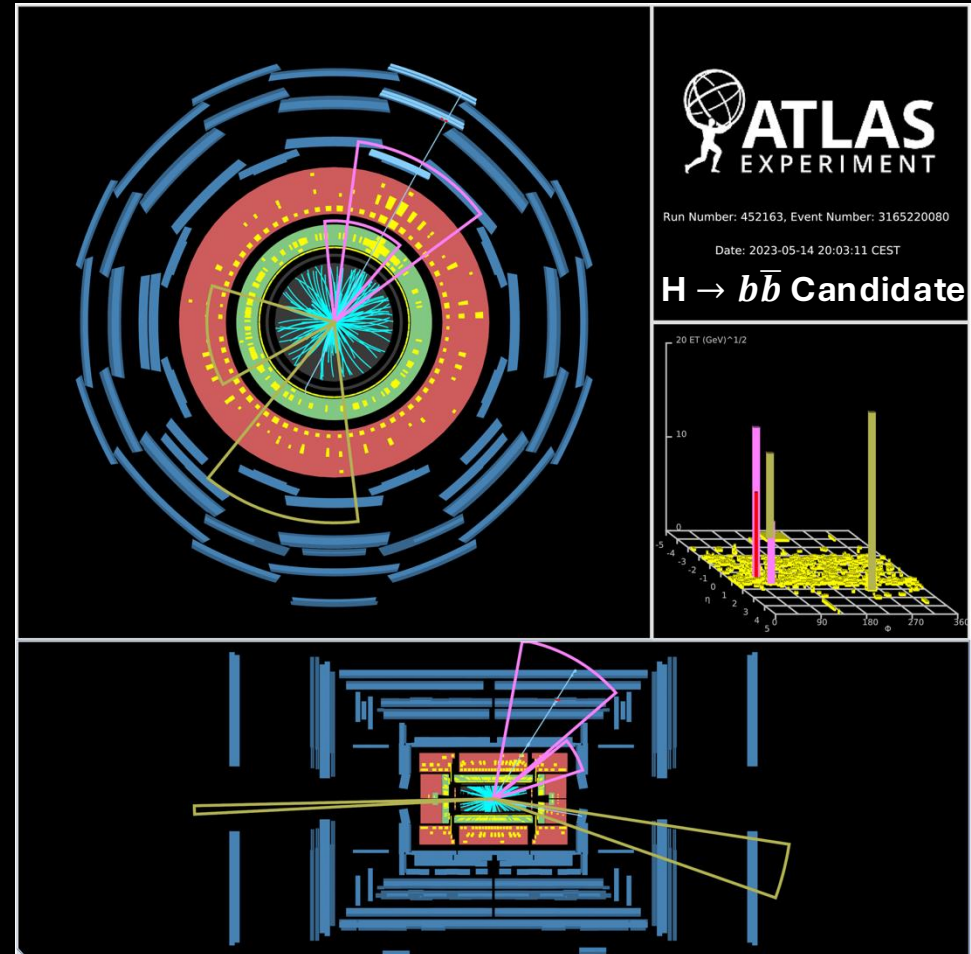
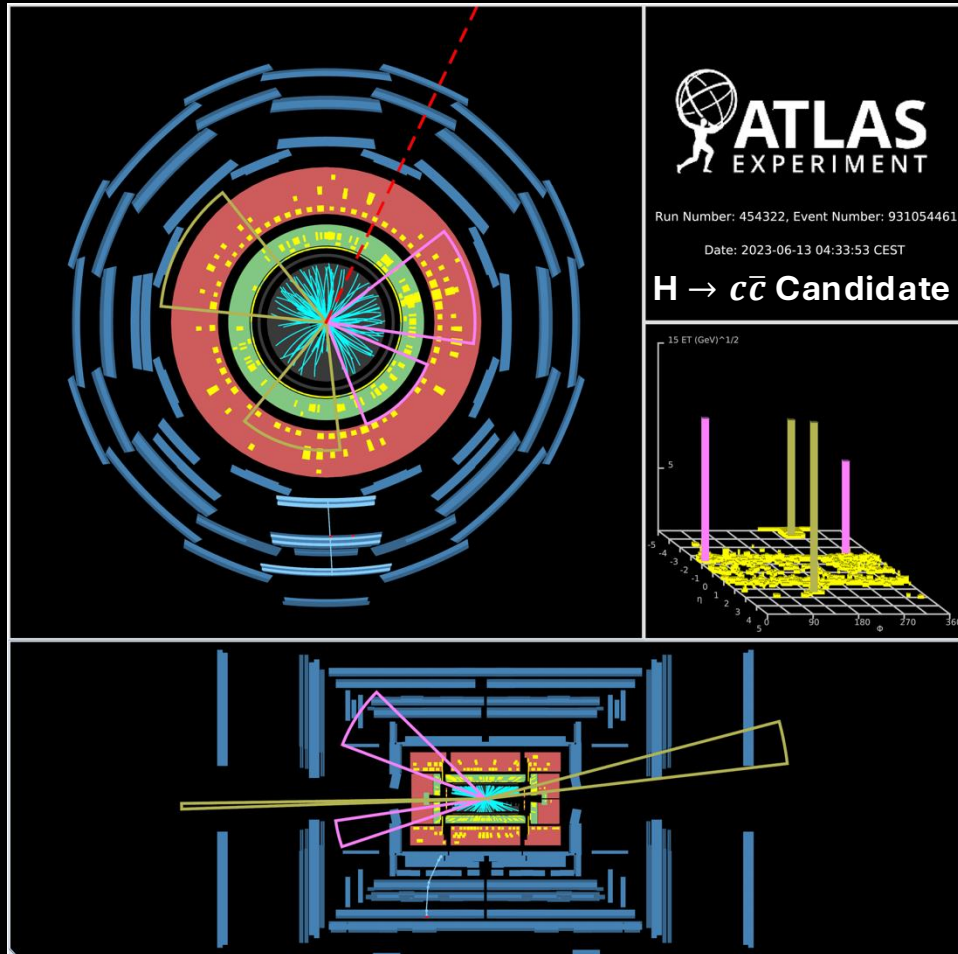
Conclusion

- ❖ First search for $H \rightarrow c\bar{c}$ in the VBF production mode.
- ❖ Evidence of $H \rightarrow b\bar{b}$ in the VBF production mode, **Observed (Expected)** significance of $\mu(H \rightarrow b\bar{b})$: **3.2 σ (3.6 σ)** when combining result with previous Run 2 VBF and VBF(+ γ) $H \rightarrow b\bar{b}$ measurements.
- ❖ Improved statistics with the inclusion of 2024-2026 will provide major improvements (**statistics prove to be the largest source of uncertainty**).



Nearly as much as
→ collected in
2018+2022+2023!

Thank You for Your Attention!



Backup

List of Uncertainties



Source of uncertainty	$\sigma(\mu^{c\bar{c}})$	$\sigma(\mu^{b\bar{b}})$
Total	13	0.53
Statistical	12	0.45
Data statistical	8.7	0.32
Non-res. bkgd normalization	4.9	0.19
Non-res. bkgd shape	4.6	0.20
Non-res. bkgd residual uncertainty	1.4	0.05
Other Higgs signal normalization	0.3	0.01
Systematic	6.5	0.28
Non-res. bkgd bias uncertainty	5.8	0.19
Simulation sample sizes	3.4	0.21
Experimental	1.8	0.18
Jet	1.8	0.18
Flavor tagging	0.3	0.01
Trigger	0.3	0.02
Other	0.06	0.02
V+jets and $t\bar{t}$ background estimate	0.7	0.03
Signal theory	0.8	0.04

Input Variables Used in ANN Training



Variable	$H \rightarrow c\bar{c}$ $H \rightarrow b\bar{b}$		Description
m_{jj}	✓	✓	Invariant mass of the VBF candidate jet pair.
$p_{T,jj}$	✓	✓	Transverse momentum of the VBF candidate jet pair.
$p_{T,j_h j_h}$	✓	✓	Transverse momentum of the Higgs jet pair.
p_T^{balance}	✓	✓	The ratio of the vectorial to scalar sums of the transverse momenta of j_{h1} , j_{h2} , j_1 and j_2 .
$\theta_{j_h j_h}$	✓	✓	Defined as $\tan^{-1} \left[\tan \left(\frac{\Delta\eta(j_h j_h)}{2} \right) / \tanh \left(\frac{\Delta\phi(j_h j_h)}{2} \right) \right]$, a measure of the relative angle of $\Delta\eta$ and $\Delta\phi$ between the two tagged jets.
$n_{\text{Jets}}^{\text{Rap}}$	✓	✓	The number of jets with $p_T > 20$ GeV and η between η_{j_1} and η_{j_2} .
$ \Delta\phi(j_h j_h, jj) $	✓	✓	The separation in ϕ between the Higgs jet pair and the VBF candidate jet pair.
$N_{\text{trk}}^{j_1}$	✓	✓	The number of tracks matched to the leading VBF candidate jet.
$N_{\text{trk}}^{j_2}$	✓	✓	The number of tracks matched to the sub-leading VBF candidate jet.
$D_{\text{GN2}}^{j_{h1}}$	✓		Binned output of the GN2 tagging algorithm for the leading c -tagged jet, with bin boundaries corresponding to 50%, 30%, and 10% c -tagging efficiencies.
$D_{\text{GN2}}^{j_{h2}}$	✓		Binned output of the GN2 tagging algorithm for the sub-leading c -tagged jet, with bin boundaries corresponding to 50%, 30%, and 10% c -tagging efficiencies.
p_T^{AddJet}		✓	Transverse momentum of the additional jet with the highest transverse momentum that does not belong to either the VBF candidate jets or the Higgs jets, and satisfies $ \eta < 2.5$. If no such jet exists, the value is set to 0 by default.

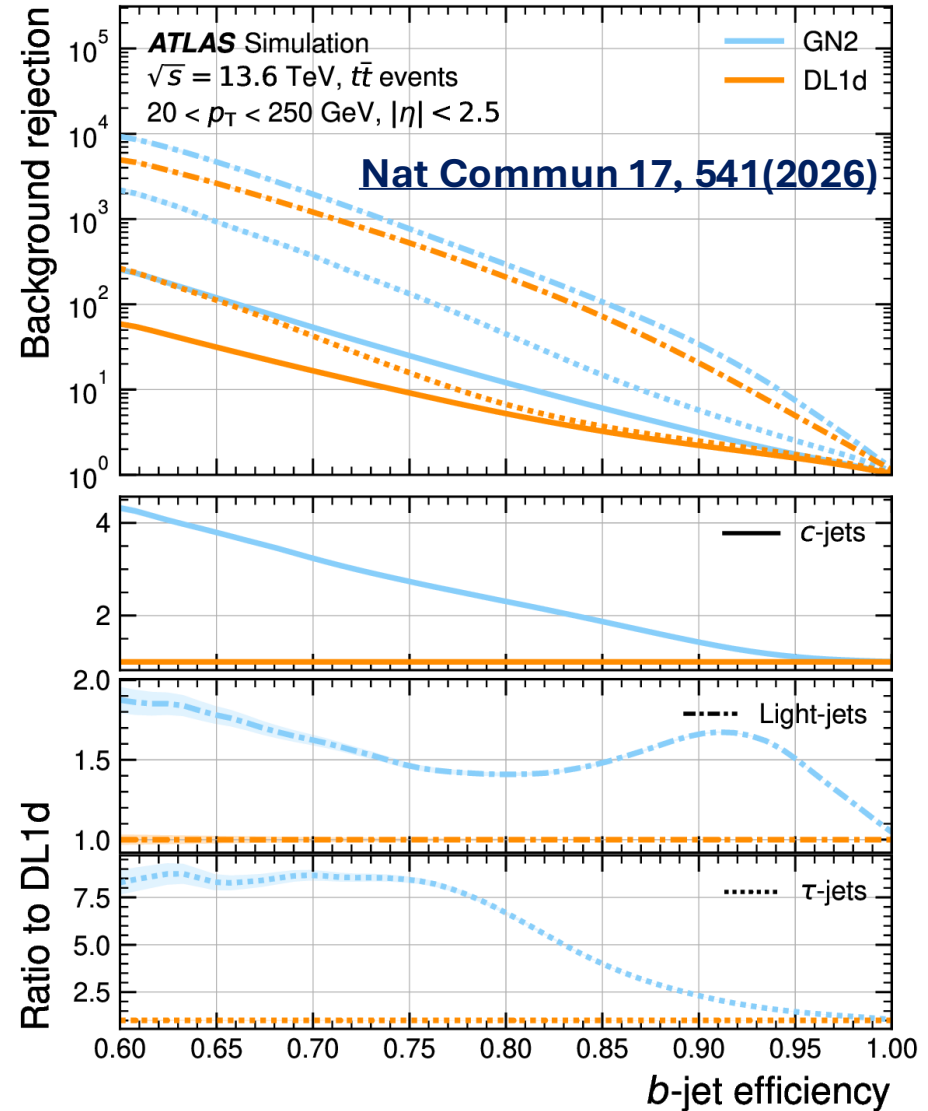
Improvements in Flavour Tagging

1

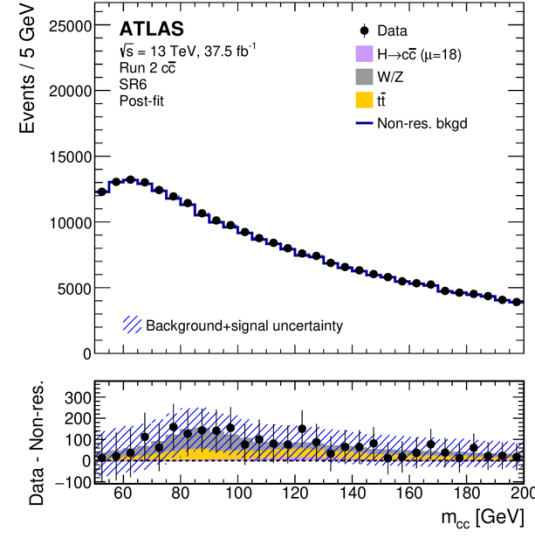
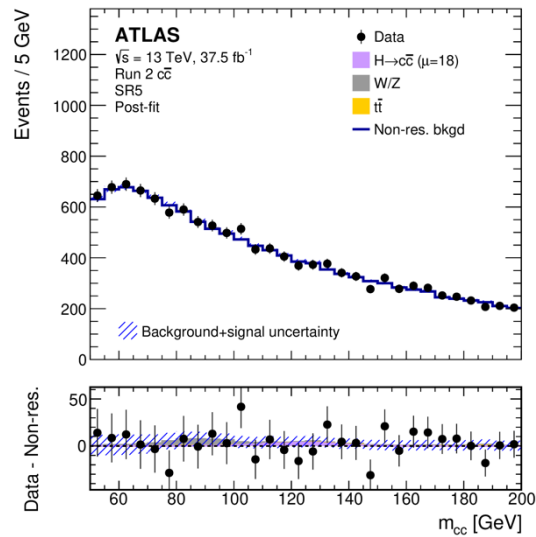
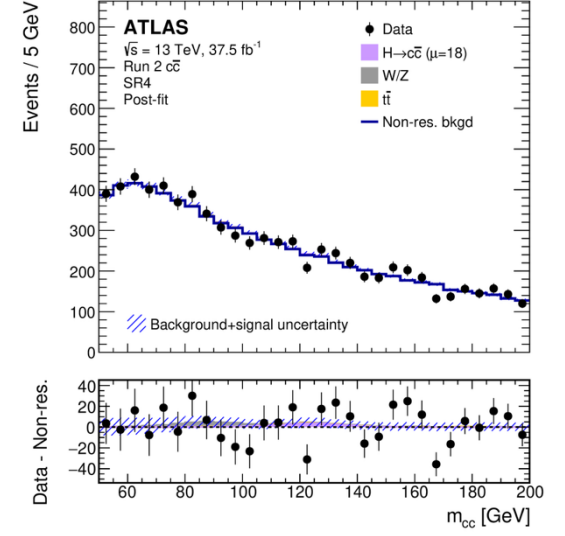
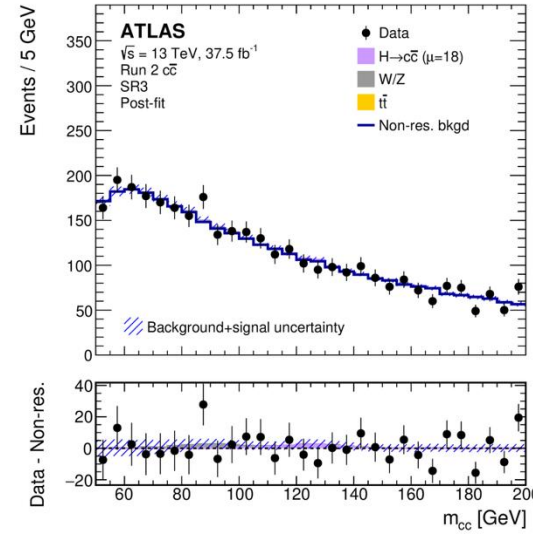
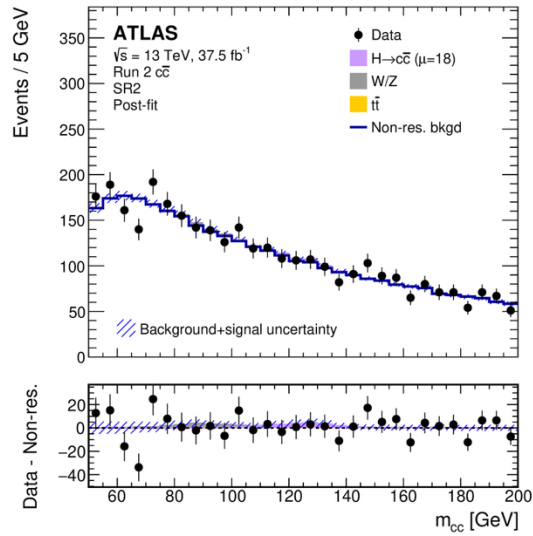
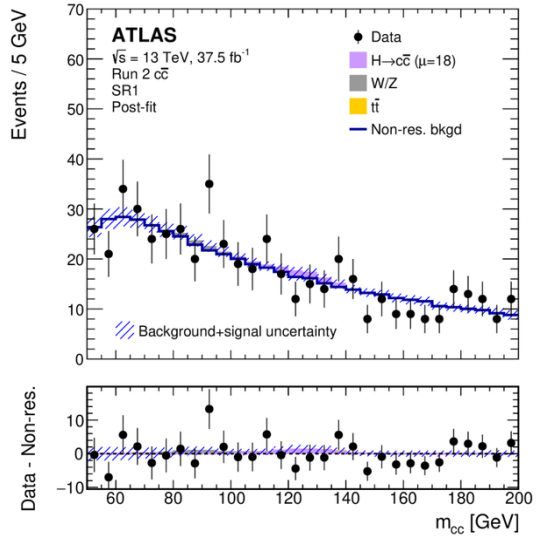


b-jet efficiency ROC curves

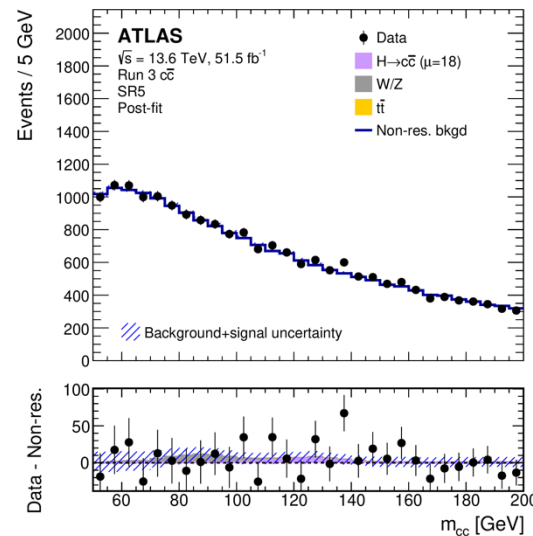
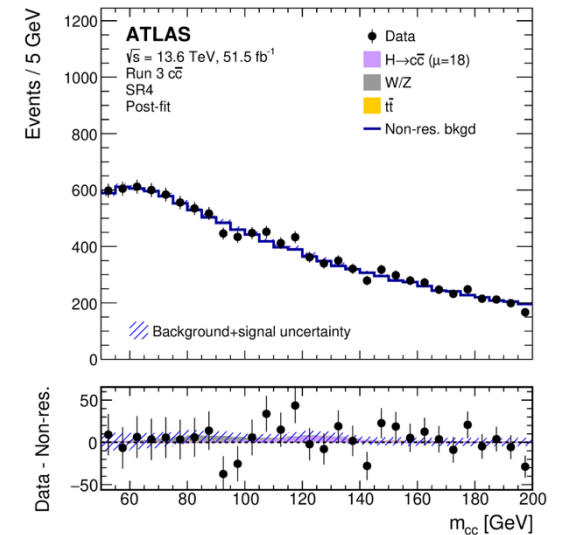
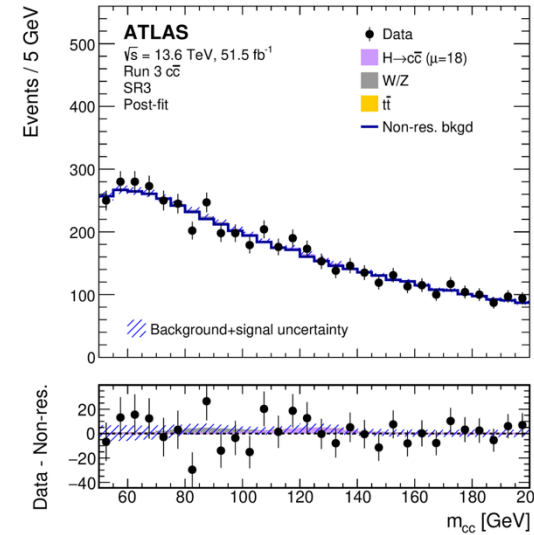
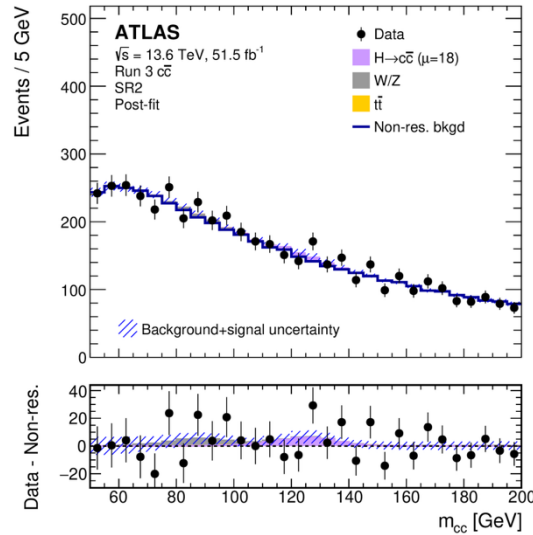
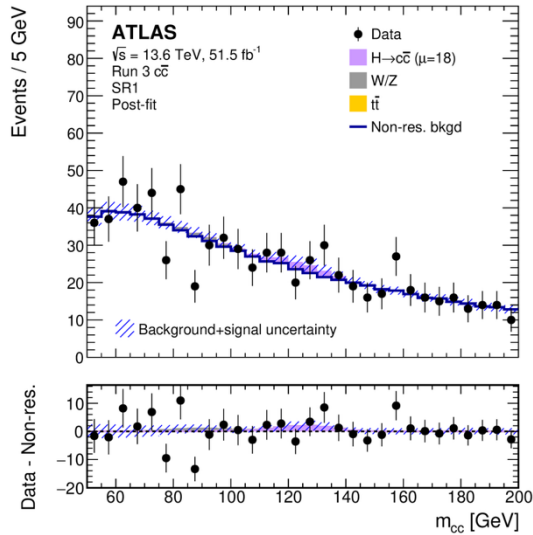
demonstrating GN2's background rejection of c-jets (solid), light-jets (dotted-dashed), and τ -jets (dashed).



Post Fit Distributions - $H \rightarrow c\bar{c}$ Run 2



Post Fit Distributions - $H \rightarrow c\bar{c}$ Run 3



Post Fit Distributions - $H \rightarrow b\bar{b}$ Run 3

